Received: 13 December 2019 | Revised: 13 August 2020 | Accepted: 14 August 2020

DOI: 10.1111/mec.15608

ORIGINAL ARTICLE

MOLECULAR ECOLOGY WILEY

Global gene expression patterns in *Porites* white patch syndrome: Disentangling symbiont loss from the thermal stress response in reef-building coral

Carly D. Kenkel[1] | Veronique J. L. Mocellin[2] | Line K. Bay[2]

[1]Department of Biological Sciences, University of Southern California, Los Angeles, CA, USA

[2]Australian Institute of Marine Science, Townsville, Qld, Australia

Correspondence
Carly D. Kenkel, Department of Biological Sciences, University of Southern California, 3616 Trousdale Parkway, Los Angeles, CA 90089, USA.
Email: ckenkel@usc.edu

Funding information
Division of Biological Infrastructure, Grant/Award Number: 1401165

Abstract

The mechanisms resulting in the breakdown of the coral symbiosis once the process of bleaching has been initiated remain unclear. Distinguishing the process of symbiont loss from the thermal stress response may shed light on the cellular and molecular pathways involved in each process. This study examined physiological changes and global gene expression patterns associated with white patch syndrome (WPS) in *Porites lobata*, which manifests in localized bleaching independent of thermal stress. In addition, a meta-analysis of global gene expression studies in other corals and anemones was used to contrast differential regulation as a result of disease and thermal stress from patterns correlated with symbiotic state. Symbiont density, chlorophyll *a* content, holobiont productivity, instant calcification rate, and total host protein content were uniformly reduced in WPS relative to healthy tissue. While expression patterns associated with WPS were secondary to fixed effects of source colony, specific functional enrichments combined with a lack of immune regulation suggest that the viral infection putatively giving rise to this condition affects symbiont rather than host cells. Expression in response to WPS also clustered independently of patterns in white syndrome impacted *A. hyacinthus*, further supporting a distinct aetiology of this syndrome. Expression patterns in WPS-affected tissues were significantly correlated with prior studies that examined short-term thermal stress responses independent of symbiotic state, suggesting that the majority of expression changes reflect a nonspecific stress response. Across studies, the magnitude and direction of expression change among particular functional enrichments suggests unique responses to stressor duration and highlights distinct responses to bleaching in an anemone model.

KEYWORDS

bleaching, coral, meta-analysis, *Porites lobata*, symbiosis, Tag-Seq

1 | INTRODUCTION

Dinoflagellates in the family Symbiodiniaceae are obligate endosymbionts of reef-building corals. Photosynthetically-derived nutrition provided by symbionts largely fuels the process of coral host calcification which builds the three dimensional reef structure that supports ecosystem function (Oakley & Davy, 2018; Rogers, Blanchard, & Mumby, 2014). Host energetic status, calcification, and consequently, ecosystem function are impaired in the process known as

'coral bleaching' in which abiotic stress leads to the breakdown of the symbiosis. Thermal stress events are the most common cause of mass bleaching worldwide and are increasing in frequency and severity as a result of global climate change (Hughes et al., 2018). Resolving the mechanisms that facilitate initiation and maintenance of a healthy symbiosis, as well as those underpinning its breakdown will be essential for developing solutions to the ongoing coral reef crisis (Weis, 2019).

A number of biological processes are thought to be involved in mediating the establishment and long-term maintenance of the coral symbiosis including host-microbe signaling, regulation of the host innate immune response and cell cycle, phagocytosis, and cytoskeletal rearrangement (Davy, Allemand, & Weiss, 2012). Five different bleaching mechanisms have been observed and/or proposed, including exocytosis of symbionts, in situ degradation, host cell detachment, host cell apoptosis, and host cell necrosis, but it is unknown which mechanism(s) predominate in natural bleaching events, whether mechanisms differ among species, and to what extent they may interact (reviewed in Oakley & Davy, 2018; Weis, 2008). A comparative study which exposed clonal replicates of *Aiptasia pallida* to a combination of controlled abiotic stressors found that expulsion of intact symbionts from host cells was the predominant response to heat and/or light stress, while in situ degradation of symbiont cells and host-cell detachment also played a role in the bleaching response to acute cold shock (Bieri, Onishi, Xiang, Grossman, & Pringle, 2016). An earlier study, however, reported that host cell detachment was the predominant mechanism of bleaching in response to elevated temperature stress (Gates, Baghdasarian, & Muscatine, 1992), whereas in situ degradation of symbiont cells was the primary response of a temperate coral to annual thermal bleaching (Ainsworth & Hoegh-Guldberg, 2008). It is possible that these mechanisms may occur in combination depending on the magnitude and duration of the stress (Bieri et al., 2016; Gates et al., 1992), but work is needed to quantify their relative importance (Oakley & Davy, 2018).

High-throughput transcriptomic, proteomic, and metabolomic approaches have provided additional mechanistic insight into the cellular functions which are disrupted as a result of thermal stress and bleaching. Unfolded protein and oxidative stress response pathways have been universally highlighted regardless of the experimental approach (Barshis et al., 2013; Cziesielski et al., 2018; Oakley et al., 2016). Transcriptomic and proteomic studies have also repeatedly identified changes to cytoskeleton and extracellular matrix proteins (DeSalvo, Sunagawa, & Voolstra, 2010; DeSalvo et al., 2008; Oakley et al., 2016), which has been interpreted as evidence supporting the role of autophagy and apoptosis in the mechanism of bleaching (Oakley & Davy, 2018). However, other investigations into thermal stress responses of aposymbiotic juvenile coral life history stages have also identified differential regulation of cytoskeletal components and heat shock proteins (Meyer, Aglyamova, & Matz, 2011; Polato et al., 2010; Rodriguez-Lanetty, Harii, & Hoegh-Guldberg, 2009; Voolstra, Schnetzer, et al., 2009), suggesting that these responses are not necessarily unique to the process of bleaching, but rather reflect a more general cellular stress response common to all organisms (Kültz, 2005). Consequently, disentangling the thermal stress response from the process of symbiont loss may help distinguish among the prospective cellular and molecular mechanisms responsible for bleaching.

The coral symbiosis can break down in response to a variety of stressors, both biotic and abiotic (Brown & Howard, 1985); however, few studies have examined molecular or cellular responses to bleaching in nonheat related contexts. Pharmacological agents can be used to induce bleaching independent of temperature, and indeed, host cell detachment has been observed in response to chemical stress (Sawyer & Muscatine, 2001). It is also possible to bleach facultatively symbiotic *Aiptasia pallida* anemones using menthol without impairing their ability to later re-establish symbiosis (Matthews et al., 2016). A proteomic comparison of symbiotic and aposymbiotic anemones generated via menthol bleaching identified an increase in proteins involved in mediating reactive oxygen stress (Oakley et al., 2016). Oxidative stress response pathways were also differentially regulated in menthol-bleached *Aiptasia* reinfected with a heterologous symbiont type (Matthews et al., 2017), suggesting that this pathway responds, at least in part, to symbiotic state independent of ambient temperature. While some progress has been made in anemone models, to our knowledge, similar attempts to disentangle bleaching from thermal stress have yet to be undertaken in reef-building corals.

This study aimed to fill this gap by taking advantage of a coral disease which does not harm host tissue integrity but results in localized bleaching independent of thermal stress. White patch syndrome (WPS) affects massive poritids in the Indo-Pacific (Lawrence, Davy, Wilson, Hoegh-Guldberg, & Davy, 2015; Raymundo, Rosell, Reboton, & Kaczmarsky, 2005; Roff, Ulstrup, Fine, Ralph, & Hoegh-Guldberg, 2008). In corals affected by WPS, small patches of bleached tissue are present without any necrosis or apparent impact to host tissues (Lawrence et al., 2015; Roff et al., 2008). A comparative analysis of symbiont photosynthetic function in response to different coral diseases found that WPS was the only syndrome to impact symbiont photosynthetic function in a pattern similar to thermal stress induced bleaching (Roff et al., 2008). Additional physiological data revealed that patches contained significantly reduced chlorophyll *a* content, but that soluble host protein content was similar to healthy tissue, suggesting that WPS primarily impacts photosymbionts (Lawrence et al., 2015). Transmission electron microscopy images generated in the same study confirmed that while host tissue remained intact within patches, there was a significant increase in virus-like particles in both coral and Symbiodiniaceae cells, suggesting that the causative agent of WPS may be a virus which infects either the host or symbiont (Lawrence et al., 2015).

We used global gene expression analyses in combination with a suite of ecophysiological assays to compare the molecular and physiological responses of healthy and WPS tissue patches within and among eight independent coral colonies. In addition, we conducted a meta-analysis to compare and contrast WPS expression responses with prior global gene expression studies examining coral disease (Wright, Aglyamova, Meyer, & Matz, 2015), symbiotic state

(Matthews et al., 2016), short-term thermal stress in adult and aposymbiotic larval corals (Dixon et al., 2015; Meyer et al., 2011), and long-term thermal stress in adult corals (Davies, Marchetti, Ries, & Castillo, 2016). We find that all aspects of coral holobiont physiology are negatively impacted by WPS, but that global gene expression patterns associated with WPS are secondary to fixed effects of source colony. Overall, WPS expression patterns are distinct from host expression responses to disease in another coral and most similar to short-term thermal stress responses regardless of symbiotic status. Specific enrichments suggest that if WPS is caused by a viral infection as suggested by Lawrence et al. (2015), then it does not significantly alter regulation of immune-response genes in *Porites* host tissue.

2 | MATERIALS AND METHODS

2.1 | Sample collection

Eight colonies of *Porites lobata* were sampled between 19–21 April 2015 from the northern side of Pandora reef (18.813878°S, 146.432784°E) under Great Barrier Reef Marine Park Authority permit G12/35236.1 and G14/37318.1. Colonies were haphazardly selected based on exhibiting the WPS phenotype. Four cores were taken from each of eight corals that exhibited WPS symptoms: (a) two from the centre of an affected patch; and (b) two from an adjacent area of normal tissue using an underwater drill (18V Nemo Power Tools, USA) fitted with a custom-built 2 cm diameter coring attachment with diamond tip teeth. One core of each origin was snap frozen in liquid nitrogen after collection for RNA analysis. The second core was held in an onboard flow-through seawater system with source water from the collection site prior to being photographed and assessed for photosynthesis and respiration capability. Once respirometry measures were complete the second core was also snap frozen for further physiological analyses in equal conditions, approximately 6 hr after collection.

2.2 | Physiological assays

Net photosynthesis and respiration were assayed on the day of collection following the two-point method originally described and validated for *A. millepora* (Strahl et al., 2015). Cores were incubated for 100 min at either 250 μmol/photon/m^2/s (net photosynthesis) or full darkness (respiration). During incubations each core was enclosed in a 600 ml acrylic chamber filled with unfiltered seawater from the collection site, placed onto custom built tables with rotating magnets, which served to power stir bars within each chamber to facilitate water mixing. To account for potential changes in oxygen content due to the metabolic activity of other microorganisms in the seawater, two chambers without corals were used as blanks in each run. At the end of the incubation period the O_2 concentration of the seawater in each chamber was measured using a hand-held dissolved oxygen meter (HQ30d, equipped with LDO101 IntelliCAL oxygen probe, Hach, USA). Values from blank chambers were subtracted from measures made in coral chambers and the subsequent rate of net photosynthesis was related to coral surface area, calculated in μg O_2/cm^2/min. Gross photosynthesis was calculated as the sum of net photosynthesis and respiration. Holobiont productivity (P:R) was quantified as the ratio of oxygen production (gross photosynthesis) to oxygen consumption through respiration.

To determine total alkalinity, a 120 ml subsample of seawater from each incubation chamber was fixed immediately following the light incubation with 0.5 mg mercuric chloride (final concentration 4 mg/L). Light calcification rates were determined from changes in alkalinity quantified with the alkalinity anomaly technique (Chisholm & Gattuso, 1991) using a Titrando 855 Robotic Titrosampler (Metrohm AG, Switzerland). Values from blank chambers were subtracted from measures made in coral chambers and calcification rate was related to coral surface area and calculated in μM $CaCO_3$/cm^2/min.

To quantify symbiont density, photosynthetic pigments and protein content, tissues were removed from host skeletons using an air gun and 0.2 μM filtered seawater (FSW) and homogenized for 60 s using a Pro250 homogenizer (Perth Scientific Equipment, AUS). Coral skeletons were rinsed with 5% bleach then dried at room temperature. Skeletal surface area was quantified using the single wax dipping method (Stimson & Kinzie, 1991) and skeletal volume was determined by calculating water displacement in a graduated cylinder. A 200 μl aliquot of tissue homogenate was fixed with equal volume of 10% formalin in FSW and used to quantify *Symbiodiniaceae* cell density. The average cell number was obtained from four replicate haemocytometer counts of a 1 mm^3 area and cell density was related to coral surface area and expressed as cells/cm^2. A 1 ml aliquot of the tissue homogenate was centrifuged for 3 min at 1,500 *g* at 4°C and the pellet was stored at −80°C for chlorophyll analysis. The remaining homogenate was separated into host and symbiont fractions by cold centrifugation (4°C) for 10 min at 3,200 *g*. To quantify chlorophyll concentrations, algal pellets were resuspended in 1 ml chilled 95% Ethanol for absorbance measurements. The homogenate was sonicated on ice for 30 s at 40% amplitude and centrifuged for 5 min at 10,000 *g* at 4°C. A 200 μl aliquot of sample extract was loaded to a 96-well plate, and absorbance was recorded at 632, 649, and 665 nm. Chlorophyll *a* concentration was calculated using the equation in Ritchie (2008), normalized to surface area, and expressed as μg/cm^2. A commercial colorimetric protein assay kit (DCTM Protein Assay Kit, Bio-Rad, Hercules, USA) was used to quantify total protein content of the coral host tissue. A 50 μl aliquot of host tissue supernatant was digested using 50 μl 1 M sodium hydroxide for 1 hr at 90°C. The plate was centrifuged for 3 min at 1,500 *g*. Following manufacturer's instructions, 5 μl of digested tissue was mixed with 25 μl alkaline copper tartrate solution and 200 μl dilute Folin reagent in a 96-well plate. Absorbance at 750 nm was recorded after a 15 min incubation. Sample protein concentrations were calculated using a standard curve of bovine serum albumin ranging from 0 and 2,000 μg/ml. Protein concentrations were normalized to total homogenate volume and coral surface area and expressed as mg/cm^2.

2.3 | Tag-seq library preparation

Total RNA was extracted using an Aurum Total RNA mini kit (Bio-Rad, CA), with minor modifications. Tissue was scraped from the surface of frozen samples and immediately homogenized in lysis buffer using a razor blade and back-pipetting following Kenkel et al., (2011). Homogenates were kept on ice for 1 hr with occasional vortexing to increase RNA yields, which was followed by centrifugation for 2 min at 14,000 *g* to precipitate skeleton fragments and other insoluble debris; 700 µl of the supernatant was used for RNA purification. At the final elution step, the same 25 µl of elution buffer was passed twice through the spin column to maximize both yield and concentration of eluted RNA. Samples were DNAse treated as in Kenkel et al. (2011). One µg of total RNA per sample was used for tag-based RNA-seq, or Tag-Seq (Meyer et al., 2011), with modifications for sequencing on the Illumina platform. The current versions of the laboratory and bioinformatic protocols for Tag-Seq are maintained at https://github.com/ckenkel/tag-based_RNAseq. Tag-Seq has been shown to generate more accurate estimates of protein-coding transcript abundances than standard RNA-seq, at a fraction of the cost (Lohman, Weber, & Bolnick, 2016).

2.4 | Reference transcriptome sequencing, assembly and annotation

To generate a *P. lobata* reference transcriptome, five replicate fragments of a single coral colony were subject to a 2-week temperature stress experiment as described in (Kenkel & Bay, 2018). Snap frozen samples from control (27°C, days 4 and 17) and heat (31°C, days 2, 4 and 17) treatments were crushed in liquid nitrogen and total RNA was extracted using an Aurum Total RNA mini kit (Bio-Rad, CA). RNA quality and quantity were assessed using the NanoDrop ND-200 UV-Vis Spectrophotometer (Thermo Scientific, MA) and gel electrophoresis. RNA samples from replicate fragments were pooled in equal proportions and 1.1 µg was shipped on dry ice to the Oklahoma Medical Research Foundation NGS Core where Illumina TruSeq Stranded libraries were prepared and sequenced on one lane of the Illumina Hiseq 3000/4000 to generate 2 × 150 PE reads.

Sequencing yielded 76 million raw PE reads. The *fastx_toolkit* (http://hannonlab.cshl.edu/fastx_toolkit) was used to discard reads < 50 bp or having a homopolymer run of 'A' ≥9 bases, retain reads with a PHRED quality of at least 20 over 80% of the read and to trim TruSeq sequencing adaptors. PCR duplicates were then removed using a custom perl script (https://github.com/ckenkel/annotatingTranscriptomes). Remaining high quality filtered reads (19 million paired reads; 3 million unpaired reads) were assembled using Trinity v 2.0.6 (Grabherr et al., 2011) using the default parameters and an in silico read normalization step at the Texas Advanced Computing Center (TACC) at the University of Texas at Austin.

The holobiont assembly was filtered to produce a host-specific assembly using a series of hierarchical BLAST searches against the *Acropora digitifera* (Shinzato et al., 2011) and *Symbiodinium kawagutii* (Lin et al., 2015) proteomes, and NCBI's nr database (Pruitt, Tatusova, & Maglott, 2005) following (Kenkel & Bay, 2017). Annotation was performed following the protocols and scripts described at https://github.com/ckenkel/annotatingTranscriptomes. Contigs were assigned putative gene names and gene ontologies using a BLASTx search (*E* value <= 10^{-4}) against the UniProt Knowledgebase Swiss-Prot database (UniProt Consortium, 2015). KOG (EuKaryotic Orthologous Groups) annotations were computed using eggnog-mapper (Huerta-Cepas et al., 2017) based on eggNOG 4.5 orthology data (Huerta-Cepas et al., 2016) and KEGG (Kyoto Encyclopedia of Genes and Genomes) id's using the KAAS server (http://www.genome.jp/kegg/kaas/ Moriya, Itoh, Okuda, Yoshizawa, & Kanehisa, 2007). The stats.sh command of the BBMAP package (Bushnell, 2014) was used to calculate GC content of host transcriptomes. Transcriptome completeness was evaluated through comparison to the Benchmarking Universal Single-Copy Orthologue (BUSCO v2) (Simão, Waterhouse, Ioannidis, Kriventseva, & Zdobnov, 2015) set using the gVolante server (https://gvolante.riken.jp/analysis.html).

2.5 | Tag-seq sequencing

Sixteen Tag-Seq libraries were sequenced across four lanes of the HiSeq 2500 at the University of Texas at Austin Genome Sequencing and Analysis Facility. Resulting reads were concatenated by sample before processing. On average 7.3 million sequences were generated per library (median: 5.3 million, range: 0.2–43.8 million), for a total of 117.7 million raw reads. Custom perl scripts were used to discard nontemplate sequence reads (defined as reads lacking the appropriate sequencing primer at the 5' end) while also trimming sequencing primers. The fastx_toolkit (http://hannonlab.cshl.edu/fastx_toolkit/index.html) and BBTools (https://sourceforge.net/projects/bbmap/) were used to further remove reads shorter than 20 bases or exhibiting homopolymer runs of "A" in excess of eight bases or those exhibiting significant matches to illumina indexes. From these, only reads with PHRED quality of at least 20 over 70% of the sequence were retained. See Table S1 for a summary of reads retained in each filtering step.

SHRiMP2 (David, Dzamba, Lister, Ilie, & Brudno, 2011) was used to map filtered reads against the *P. lobata* host reference concatenated to the *Cladocopium* strain C15 reference transcriptome (Shinzato, Inoue, & Kusakabe, 2014) as in (Kenkel, Moya, Strahl, Humphrey, & Bay, 2018). Resulting read counts were summed by isogroup (groups of sequences putatively originating from the same gene, hereafter referred to as genes), sample, and focal organism (host, symbiont). On average, 2.1 million reads per sample were mapped to 25,222 genes in the host transcriptome, while 0.7 million reads per sample were mapped to 10,629 genes in the symbiont transcriptome. Due to the low number of reads mapping

to the symbiont reference, only host expression data were statistically analysed.

2.6 | Statistical analyses of expression patterns in *P. lobata*

All statistical analyses were completed in R 3.6.0 (R Core Team, 2017) and scripts and input files can be found at https://github.com/ckenkel/PoritesWPS. For the physiological data, we modelled the fixed effect of condition (levels: healthy, WPS) on *Symbiodiniaceae* cell density, chlorophyll a content, gross photosynthesis, total host protein and holobiont instant calcification rate using the lme command of the NLME package (Pinheiro, Bates, DebRoy, & Sarkar, 2014). Source coral colony identity was included in all models as a scalar random factor. Models were assessed for normality of residuals and homoscedasticity. The prcomp command of the stats package was used to conduct a principal components analysis of the host physiology data and the first principal component was used as an additional trait for correlation with gene expression.

For gene expression counts, the package arrayQualityMetrics (Kauffmann, Gentleman, & Huber, 2009) was used to identify outliers. Both the normal and WPS samples from coral genet 4 were identified as outliers and excluded from further analysis in the host data set, probably due to the poor quality of sample 4N (the healthy sample, Table S1). Statistical analyses were conducted using the package DESEQ (Anders & Huber, 2010). A Cox-Reid adjusted profile likelihood model specifying coral colony of origin and phenotype (normal or WPS) was used to obtain the maximum dispersion estimate of the raw counts data. The bottom 10% quantile of genes was identified as the statistic which best satisfied the assumptions of independent filtering as implemented in genefilter (Gentleman, Carey, Huber, & Hahne, 2019) and these low-expression genes were removed from the data set prior to formal hypothesis testing. This left 22,630 highly expressed genes. A series of generalized linear models implemented using the function fitnbinomGLMs were used to test the effects of WPS phenotype and PC1 of the physiology data on the expression of individual genes while controlling for fixed effects of colony of origin. The KOGMWU package (Dixon et al., 2015) was used to test for rank-based enrichment of euKaryotic Orthologous Groups (KOG) terms among differentially expressed genes by WPS phenotype. The GO_MWU package (Wright et al., 2015) was used to test for rank-based enrichment of gene ontology terms. Rather than a categorical functional enrichment based on *p*-value cutoffs, these packages compute delta-ranks based on gene expression measures for each term (GO or KOG) as the difference between the mean rank of genes annotated with a specific term and the mean rank of remaining genes in the global gene set. This value reflects the degree of enrichment of a particular term among up- or downregulated genes, relative to the rest of the data set and significance is calculated using a two-sided Mann-Whitney *U* test followed by a Benjamini-Hochberg false discovery rate correction. Both enrichment tests were conducted using signed log *p*-values as the measure of interest as in (Strader, Aglyamova, & Matz, 2016).

To quantify the proportion of putative coral immunity-related genes in our data set, a list of GO terms containing any of the following words was compiled: immune, immunity, pathogen, lectin, complement, antimicrobial, melanin, complement, reactive oxygen, toll, and NF-kappaB (Table S2). While these terms were compiled based on the current mechanistic understanding of cnidarian immune pathways (Palmer & Traylor-Knowles, 2012), it is important to note that this is an active area of research and it may be worth revisiting this analysis as new mechanisms are discovered. Isogroups annotated with one or more of these 145 GO terms were summed in the whole reference transcriptome, the high-expression subset of the transcriptome that was analysed for differential expression, and the subset of differentially expressed genes by WPS phenotype, and a two-sided G-test was used to determine whether genes with these annotations were over- or underrepresented in any expression subset.

2.7 | Meta-analysis of gene expression response to disease, bleaching, and thermal stress

To distinguish molecular responses specific to symbiotic state from those associated with disease and thermal stress, KOG term enrichments from a set of prior studies were compared to our present results using the *KOGMWU* package. Comparative studies included host responses associated with white syndrome infection in *Acropora hyacinthus* (Wright et al., 2015), short-term thermal stress responses in aposymbiotic *A. millepora* larvae (5 days, Meyer et al., 2011), and symbiotic adult *A. millepora* (3 days, Dixon et al., 2015), long-term thermal stress response in symbiotic adult *Siderastrea siderea* (95 days, Davies et al., 2016), and symbiotic state independent of thermal stress in the model anemone *Aiptasia pallida* (Matthews et al., 2017). Raw count data for *A. hyacinthus* were downloaded from https://github.com/rachelwright8/Ahya-White-Syndromes and the reference transcriptome from https://matzlab.weebly.com/data--code.html. For the *S. siderea* and *A. pallida* data sets, tables of mapped read counts and reference transcriptomes and in the case of *A. pallida*, statistical R scripts, were obtained from the respective corresponding authors. *DESeq* (Anders & Huber, 2010) was used to reanalyse all supplementary data sets. The *A. hyacinthus* data set was reduced to only the disease and ahead of lesion samples as these most closely approximate the WPS and healthy tissue samples obtained for *P. lobata*. Moreover, Wright et al. (2015) found that expression profiles in unaffected tissues of diseased colonies (the "ahead of lesion" samples) were not significantly different from those observed in an unpaired set of healthy coral. The *A. pallida* reanalysis largely followed statistical methods originally described in Matthews et al. (2017) save that the categorical comparison of interest was aposymbiotic versus symbiotic anemones (as opposed to the type of symbiont hosted). The *S. siderea* reanalysis reduced the data set to the ambient versus elevated temperature comparison

only. The *A. millepora* data sets are included as example data with the *KOGMWU* package. For all supplementary data sets, KOG annotations were updated using eggnog-mapper (Huerta-Cepas et al., 2017) based on eggNOG 4.5 orthology data (Huerta-Cepas et al., 2016). Pearson correlations were calculated to evaluate similarity among up- and downregulated KOG classes across data sets.

3 | RESULTS

3.1 | White patch syndrome physiology

All physiological parameters were negatively impacted within WPS affected tissues. Symbiont density decreased by 1.5 × 10^6 cells/cm^2 on average in WPS infected tissue relative to paired healthy controls (p = .001, Figure 1a). Similarly, chlorophyll *a* content declined by 18.4 µg/cm^2 (p < .001, Figure 1b) and P:R ratios were reduced by 0.91 on average (p < .001, Figure 1c). Soluble host protein content was 256.7 mg/cm^2 lower (p = .046, Figure 1d) and calcification rate decreased by 11.7 µmol $CaCO_3$/cm^2/min in WPS affected tissue compared to healthy tissue on average. A principal components analysis revealed that overall, nearly 60% of the variation in the physiological data was driven by WPS phenotype (Figure S1a) whereas source colony effects were secondary (Figure S1b).

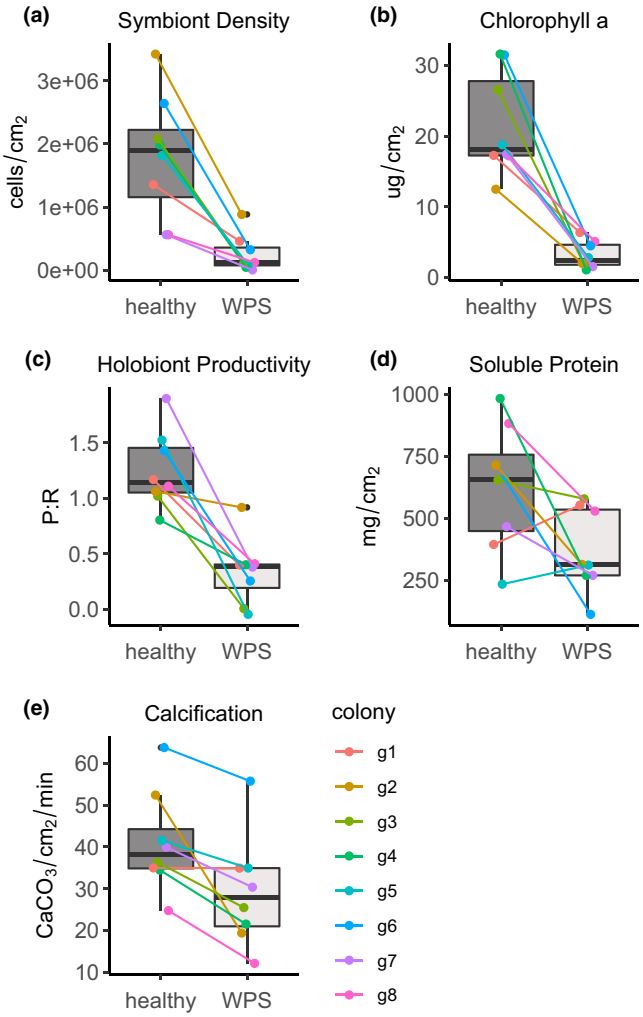

FIGURE 1 Physiological responses to white patch syndrome (WPS). Boxplots show the distribution of traits by phenotype. The median is indicated by the thick black line and the box represents the range between the upper and lower quartile. Whiskers extend maximally 1.5 times beyond the interquartile range and outliers are indicated by black circles. Coloured lines indicate paired samples originating from each unique source colony [Colour figure can be viewed at wileyonlinelibrary.com]

3.2 | Porites lobata *reference transcriptome*

The initial holobiont assembly contained 125,405 contigs over 400 bp in length (N_{50} = 1,537). Of these, 52 were discarded as matching non-mRNAs (12 rRNA, 40 mitochondrial). Following screening for biological contamination, 42,793 contigs had a best match to the *Acropora digitifera* proteome, and of these, 39,472 matched either a metazoan or had no match in NCBI's nr database. An additional 3,243 contigs matched neither proteome but exhibited a best hit to a Cnidarian in the nr database and were also retained. This *P. lobata* specific 42,715 contig assembly represented 27,436 isogroups (~genes) with an average length of 1,598 bp and an N50 of 2,147). GC content of the host-specific assembly was 42%, consistent with other anthozoan transcriptomes where *Symbiodiniaceae* reads have been effectively filtered (Kenkel & Bay, 2017; Lin et al., 2017). Protein coverage exceeded 0.75 for 43% of contigs. Of the 27,436 genes in the host transcriptome, 16,433 were annotated with gene names (59.9%) while 16,665 (60.7%) were annotated with GO terms. Comparison of this assembly to the core eukaryotic 248-gene set (Parra, Bradnam, & Korf, 2007) revealed 90.7% of KOGs were represented. Of the 978 core BUSCO gene set for metazoans (Simão et al., 2015), 89.57% were found to be complete, while an additional 2.86% were partially assembled indicating that the assembly is comprehensive, especially in comparison to other currently available resources for this species (Quek & Huang, 2019).

3.3 | Host expression associated with WPS

Unlike the physiological data, the largest effect detected in the expression data set was source colony identity. Nearly 43% of genes in the host transcriptome (9,705) were significantly differentially expressed by source colony identity, whereas only 0.7% (148 genes) were differentially expressed by WPS phenotype alone (P_{adj} < 0.1, Figure S2). An additional 396 genes (1.7%) showed an effect of both source colony and WPS. No genes exhibited significant correlations with the first principal component of the physiological data alone (PC1: Figure S2), but 10 genes showed a significant effect of WPS and PC1, while 31 genes were differentially expressed by source colony, WPS and PC1. A principal components analysis of the most significantly differentially expressed genes ranked by *p*-value confirmed that source colony identity was the major driver of variation

in expression (PC1), but PC2 largely differentiated samples based on WPS phenotype, indicating that this condition is still a reasonably strong driver of host expression (Figure S3). Of all the 585 genes exhibiting differential expression by WPS phenotype (Figure S2) the direction of regulation was fairly evenly split, with 323 genes downregulated and 255 upregulated.

Rank-based functional enrichment analyses of expression changes associated with WPS highlight a general downregulation of mitochondrial metabolism, and upregulation of both cytoskeletal components and genes involved in RNA processing and chromatin organization. Significant gene ontology (GO) enrichments were detected for biological process and cellular component terms (Figure 2). The strongest enrichments were among cellular component terms, with cytoskeletal part showing the most significant upregulation (GO:0044430, $P_{adj} < 0.001$) and mitochondrial part exhibiting the strongest downregulation (GO:0044429, $P_{adj} < 0.001$, Figure 2b). Biological process terms were less strongly regulated, but chromatin organization topped upregulated terms (GO:0006325, $P_{adj} < 0.001$) whereas regulation of ossification was the most significant enrichment among downregulated genes (GO:0030278, $P_{adj} < 0.01$). Similarly, the top three eukaryotic orthologous group (KOG) enrichments included 'energy production and conversion' ($P_{adj} < 0.001$), 'cytoskeleton' ($P_{adj} < 0.001$) and RNA processing and modification ($P_{adj} < 0.005$, Figure 3). Differentially expressed genes annotated with the energy production and conversion term largely consisted of cytochrome oxidase subunits and other enzymes in the citric acid cycle and exhibited patterns of downregulation in WPS-affected tissues (Figure S4) consistent with GO term enrichments.

Immune-related ontology terms were not enriched among either up- or downregulated genes. However, genes exhibiting low expression variance were filtered from the data set prior to testing for differential expression. To determine whether underrepresentation of immune-related genes in our data set could explain the apparent lack of immune regulation we conducted a categorical functional enrichment analysis of genes annotated with immune-related GO terms (Table S2) in the entire host transcriptome relative to the analysed subset as well as the differentially expressed subset. The proportion of genes annotated with immune-related terms was not significantly different in the analysed portion of the transcriptome relative to the global reference (Table 1). Nor did we detect any enrichment of immune-related genes among the 576 genes differentially regulated by WPS phenotype (Table 1).

3.4 | Meta-analysis of expression in response to thermal stress and bleaching

Patterns of up- and downregulation within KOG classes were used to compare WPS expression with global gene expression data generated from symbiotic adult *A. hyacinthus* exhibiting tissue loss consistent with white syndrome (Wright et al., 2015), a coral disease that has been attributed to infection by *Vibrio* spp. (Sussman, Willis, Victor, & Bourne, 2008); symbiotic adult *A. millepora* colonies in response to 3 days of heat stress (31.5°C, Dixon et al., 2015); aposymbiotic *A. millepora* larvae after 5 days of heat stress (31.4°C, Meyer et al., 2011); symbiotic adult *S. siderea* colonies after 95 days of heat

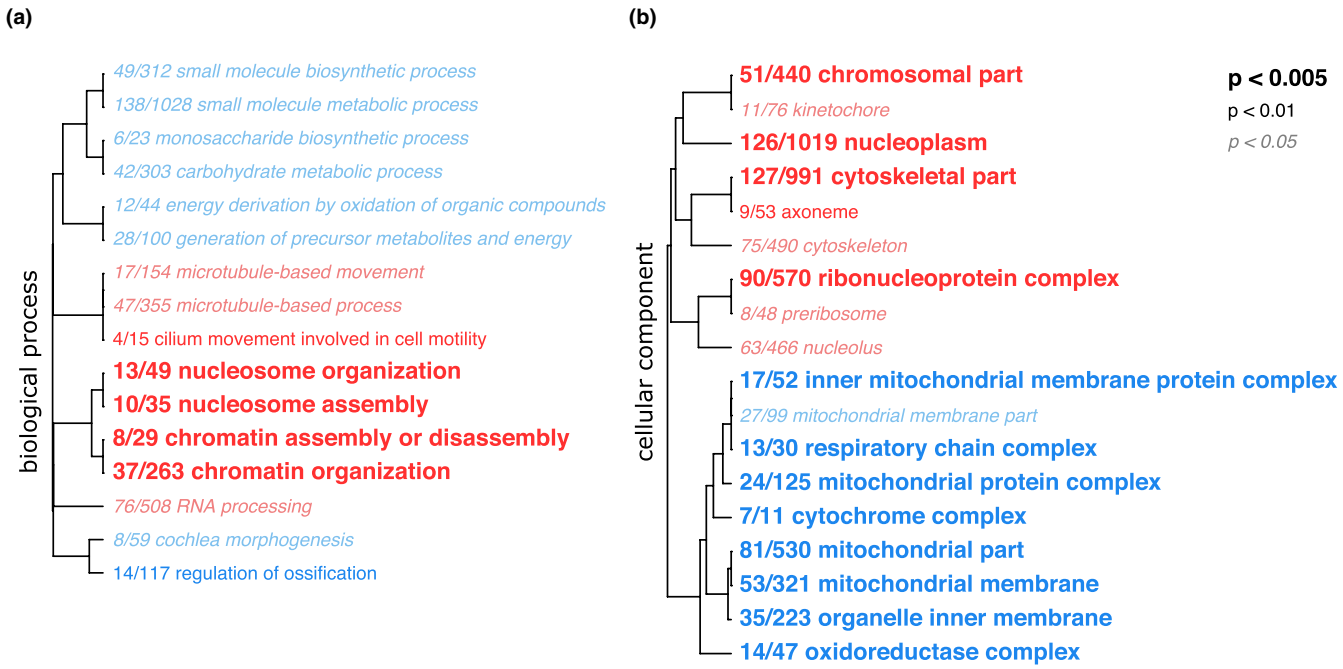

FIGURE 2 Hierarchical clustering of enriched (a) biological process; and (b) cellular component gene ontology terms among generally upregulated (red) and downregulated (blue) genes in the coral host with respect to WPS phenotype. Font size indicates the level of FDR-adjusted statistical significance. Term names are preceded by a fraction indicating the number of individual genes within each term that are differentially regulated with respect to WPS phenotype (*unadjusted p* < .05)

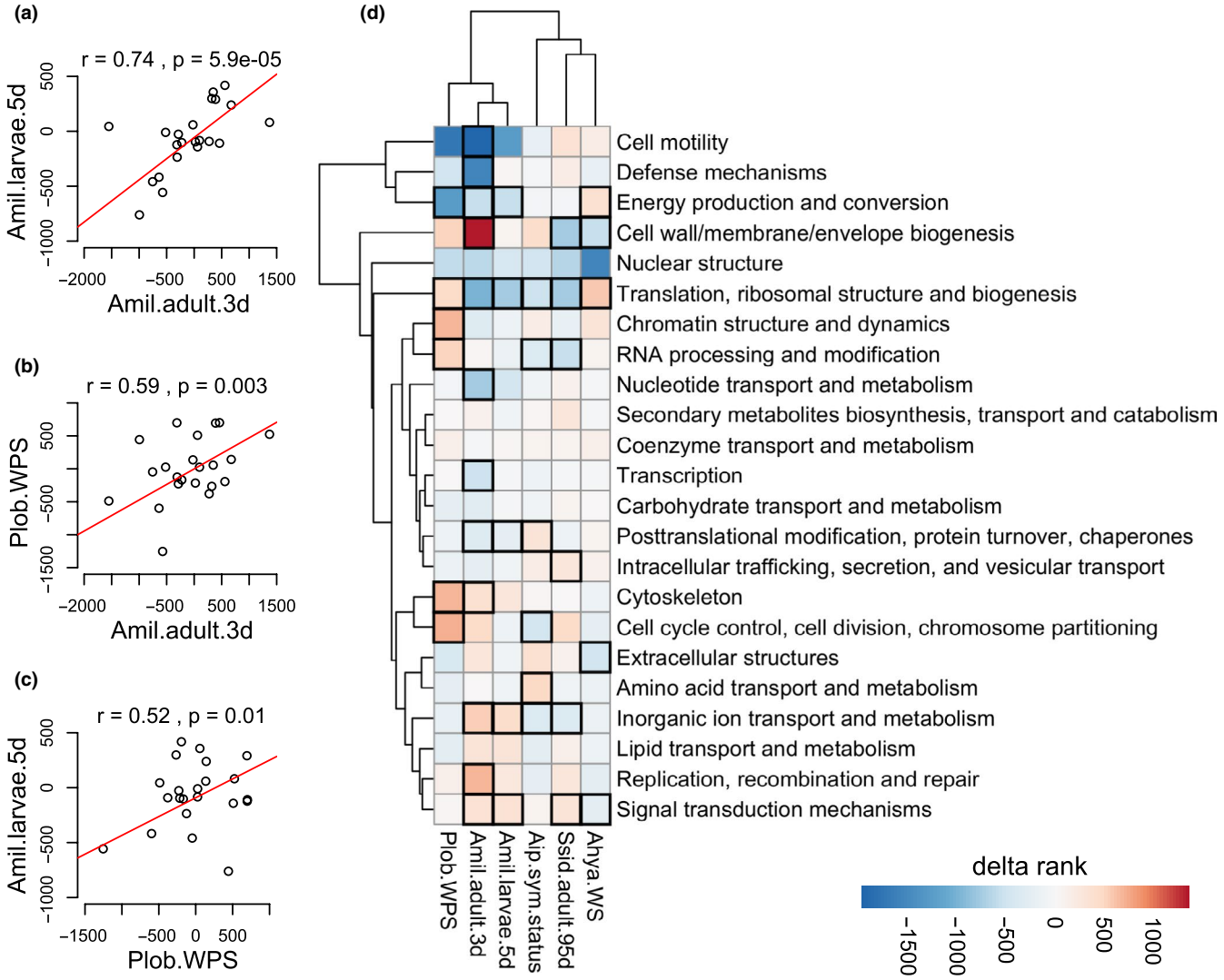

FIGURE 3 Hierarchical clustering analysis of KOG term enrichments. Correlations of KOG delta ranks between: (a) *A. millepora* larvae in response to 5-day thermal stress and adults in response to 3-day thermal stress; (b) the WPS phenotype in *P. lobata* and 3-day thermal stress in adult *A. millepora*; and (c) the WPS phenotype in *P. lobata* and 5-day thermal stress in larval *A. millepora*. (d) Shared KOG term enrichments (rows) among generally upregulated or downregulated genes (delta rank heatmap) in all data sets (column). Boxes outlined in bold are statistically significant enrichments (FDR-adjusted $p < .05$) within each data set. Aip.sym.status, menthol-bleached aposymbiotic versus symbiotic *Aiptasia*; Ssid.adult.95d, symbiotic adult *S. siderea* colonies after 95 days of heat stress; Ahya.WS, symbiotic adult *A. hyacinthus* exhibiting tissue loss consistent with white syndrome

stress (32°C, Davies et al., 2016); and menthol-bleached aposymbiotic versus. symbiotic *Aiptasia* (Matthews et al., 2017). A hierarchical clustering analysis compared the change in magnitude and direction of differentially regulated genes within each KOG class among data sets. This analysis revealed that WPS patterns were most similar to short-term stress responses in adult and larval *A. millepora* (Figure 3). The strongest correlation was detected between *A. millepora* adults and larvae, as has been reported previously (Dixon et al., 2015, $r = 0.74$, $p < .001$, Figure 3a), but WPS expression was significantly correlated with both adult ($r = 0.59$, $p = .003$, Figure 3b) and larval ($r = 0.52$, $p = .01$, Figure 3c) patterns. No significant correlations with other data sets were detected for the *A. hyacinthus*, *Aiptasia* or *S. siderea* data sets, which clustered distinctly from the *A. millepora* and *P. lobata* data sets (Figure 3d, Figure S5). We found no evidence of systematic differences among natural collections or experimental treatment conditions that could explain this clustering pattern (Table S3).

Some unique patterns differentiating among the disease, thermal stress, and bleaching data sets were also evident. Consistent significant enrichment of terms associated with replication, transcription and translation (chromatin structure and dynamics; RNA processing and modification; cell cycle control, cell division, chromosome partitioning; translation, ribosomal structure and biogenesis) were evident among upregulated genes in WPS tissue and largely absent or differentially regulated in other nondisease data sets (Figure 3d). Interestingly, "translation, ribosomal structure and biogenesis is the only significantly enriched term among all data sets, and exhibited differences in the direction of regulation. This term was enriched

TABLE 1 The proportion of genes annotated with at least one immune-related GO term (Table S2) relative to the total number of genes with any GO annotation in the full reference transcriptome, the 22,630 gene subset analysed for differential expression, and the 576 genes differentially expressed (DEGs) by WPS phenotype

Data set	# Annotated	# Immune	%
P. lobata reference transcriptome	16,665	733	4.4%
analysed transcriptome	14,392	660	4.6%
DEGs by WPS phenotype	393	16	4.1%

among downregulated genes in the thermal stress and symbiont status data sets whereas it was enriched among upregulated genes in the two putative disease data sets. "Energy production and conversion, on the other hand, was enriched in the two disease and short-term stress data sets, but the direction of expression differed. Genes with this annotation were downregulated in response to WPS and thermal stress and upregulated in white syndrome impacted tissue in *A. hyacinthus*. Signal transduction mechanisms were enriched among upregulated genes in all thermal stress data sets regardless of the duration of stress (*A. millepora* adults and larvae and *S. siderea* adults) but no enrichments were detected for the symbiotic state data sets, whereas this term was enriched among genes downregulated in response to white syndrome in *A. hyacinthus* (Figure 3d). In symbiotic adult corals, cell wall/membrane/envelope biogenesis exhibited distinct patterns of regulation depending on the length of the thermal stress, being upregulated in *A. millepora* under short-term stress, and downregulated in *S. siderea* under long-term stress. This term was also enriched among genes downregulated in *A. hyancinthus* experiencing tissue loss associated with a white syndrome. Amino acid transport and metabolism was enriched among upregulated genes in aposymbiotic *Aiptasia*, but not strongly regulated in any of the scleractinian coral data sets. A similar pattern was detected for extracellular structures among genes downregulated in diseased *A. hyacinthus* tissue with no significant enrichments in other data sets.

4 | DISCUSSION

In corals impacted by WPS, the loss of intracellular symbionts occurs independently of thermal stress, providing a rare opportunity to investigate the cellular and molecular mechanisms differentiating each of these processes in a reef-building coral. Despite the clearly negative impact of WPS on holoboint physiology, we did not detect expression patterns indicative of an immune response in the coral host. Moreover, the meta-analysis revealed that WPS expression patterns cluster independently from another coral disease data set and are most similar to short-term thermal stress responses regardless of symbiotic status. While we identified some shared patterns of regulation, the striking variation among studies examining different stressors, exposure durations, and symbiotic states highlights the need for additional work specifically designed to disentangle these different processes.

Physiological responses to WPS are similar to those observed during thermal-stress induced bleaching (Fitt, Brown, Warner, & Dunne, 2001; Porter, Fitt, Spero, Rogers, & White, 1989). The integrity of host cells is not compromised (Lawrence et al., 2015; Roff et al., 2008), but symbiont loss is evident (Figure 1). In contrast to an earlier study (Lawrence et al., 2015), we find that soluble host protein content is significantly reduced in WPS tissues on average, and host calcification is also negatively impacted (Figure 1). However, it does not necessarily follow that host tissues are being lysed. The lack of expression change in host genes associated with an immune response (Table 1, Figures 2 and 3) suggests that this physiological response is more a consequence of symbiont loss than a response to an active infection. Prior studies examining gene expression responses to natural disease events, pathogen/parasite challenge, or immunostimulants such as lipopolysaccharides, consistently report differential expression of immune-related transcripts, including both upregulation, presumably in response to an active infection, and downregulation, which may indicate immune suppression by the pathogen/parasite (Fuess, Mann, Jinks, Brinkhuis, & Mydlarz, 2018; Fuess, Pinzón C, Weil, Grinshpon, & Mydlarz, 2017; Mohamed et al., 2018; van de Water et al., 2018; Wright et al., 2015). It is possible that WPS produces a colony-wide effect that we would not be able to detect given our within-colony sampling scheme. However, Wright et al. (2015) did analyse expression of unpaired control colonies and found that expression in response to white syndrome infection was highly localized: unaffected portions of diseased colonies were statistically indistinguishable from healthy controls in terms of their expression responses. Interestingly, a lack of differential expression has been reported during the establishment of the coral symbiosis, but only for competent strains as symbionts that failed to establish resulted in substantial alteration of normal gene expression (Voolstra, Schnetzer, et al., 2009; Voolstra, Schwarz, et al., 2009). The immediate response to heat stress also differs from longer-term bleaching phenotypes in terms of gene expression patterns. In *P. astreoides*, a congener of *P. lobata*, no significant patterns of differential expression in candidate stress response or immune genes were found in phenotypically bleached corals no longer experiencing thermal stress (Kenkel et al., 2014). Taken together, our data suggest that although WPS tissues are physiologically bleached, they are not experiencing the stress of infection. This may be because WPS is a viral infection of symbionts, as has been previously suggested (Lawrence et al., 2015). More importantly, these results add to the growing body of evidence supporting the hypothesis that the response to stress and the response to symbiotic state are different molecular processes.

The hierarchical clustering analysis of KOG term enrichments identified significant correlations between the magnitude and direction of regulation in WPS and short-term thermal stress, with patterns in *A. hyacinthus*, *S. siderea*, and *Aiptasia* being distinct and unrelated, even to each other (Figure 3). This was unexpected because

as a putative viral infection (Lawrence et al., 2015), WPS reflects a bleaching phenotype independent of thermal stress, and thermal stress responses in larval *A. millepora* are independent of symbiont status. Our initial expectation was that KOG enrichments would cluster based on stressor, with WPS being most similar to white syndrome impacted *A. hyacinthus* followed by menthol bleached *Aiptasia*, and that these nonthermal stress response and bleaching phenotypes would be distinct from the three thermal stress experiments (*A. millepora* and *S. siderea*, Figure 3d). An alternate hypothesis was that longer-term differences in symbiotic status would drive clustering, with the WPS, *A. hyacinthus*, *S. siderea*, and *Aiptasia* data sets clustering independent of the short-term thermal stress experiments. Although it is important to point out that both disease data sets (WPS and white syndrome in *A. hyacinthus*) sampled corals of opportunity, and it is unknown when symptoms first occurred in any coral in relation to the sampling time-point. Given that stress response expression patterns can be highly dynamic (Ruiz-Jones & Palumbi, 2017), future work should aim to account for sampling time to control for this potential source of variation. Nevertheless, closer examination of unique and shared patterns of differential regulation suggest that a common nonspecific cellular stress response may unite the WPS and short-term stress data sets, whereas the lack of clustering among the remaining disease and symbiont status data sets may be driven by the difference in causative mechanisms or divergent host responses to a lack of symbionts.

The broad similarity in patterns of expression in WPS and short-term thermal stress may reflect nonspecific cellular stress response mechanisms (Kültz, 2005), rather than those specific to bleaching or disease. For example, upregulation of mitochondrial proteins has been reported during infection of coral larvae with a putative parasite, *Chromera* (Mohamed et al., 2018) and white-syndrome impacted *A. hyacinthus* show a significant enrichment of "Energy production and conversion" among upregulated genes (Figure 3d). This is in contrast to the WPS and short-term thermal stress data sets where this term is enriched among downregulated genes. Downregulation of mitochondrial proteins is hypothesized to be a general mechanism for protecting cells from oxidative stress (Crawford, Wang, Schools, Kochheiser, & Davies, 1997). In corals, production of reactive oxygen species (ROS) increases during thermal stress and is hypothesized to overwhelm both host and symbiont detoxification mechanisms (reviewed in Oakley & Davy, 2018; Weis, 2008). Elevated ROS production was observed in *Emiliania huxleyi* following a viral infection (Evans, Malin, Mills, & Wilson, 2006), suggesting that ROS stress may also play a role in WPS, if excess ROS are generated by symbionts during infection. Taken together, increased ROS production may help explain the similarity in global expression patterns driving clustering in these studies, although actual quantification of ROS levels in both hosts and symbionts impacted by WPS would help confirm this hypothesis.

Differences in the causative agent may be responsible for the variation among studies (Figure 3). Bleaching in WPS potentially results from a viral infection of symbionts (Lawrence et al., 2015), whereas white syndromes are thought to be the result of a bacterial infection in host tissue (Sussman et al., 2008; Wright et al., 2015). *S. siderea* were subject to long-term exposure to elevated thermal stress (Davies et al., 2016) and *Aiptasia* were chemically bleached using menthol (Matthews et al., 2017). Unlike the response to white syndrome in *A. hyacinthus* (Wright et al., 2015), we did not detect significant enrichment of any immunity or stress response pathways in WPS tissues (Table 1, Figure 2). Furthermore, functional enrichment patterns are inconsistent with global expression patterns previously reported during viral infection. Inhibition of host cellular protein synthesis which conserves cellular resources and blunts host antiviral responses, is a hallmark of many viral infections (Dai et al., 2017). Although soluble protein content was reduced in WPS samples (Figure 1d), we observed enrichment of replication, transcription and translation among upregulated genes in the WPS data set (Figures 2 and 3). One possible explanation for these contradictory findings is that our sampling time-point occurred when cells were just reinitiating protein synthesis to facilitate cellular recovery. However the upregulation of replication, transcription and translation was a pattern which differentiated both disease data sets. Significant enrichment of translation, ribosomal structure and biogenesis occurred among upregulated genes in the WPS and *A. hyacinthus* white syndrome data sets, but among downregulated genes in every other data set. Downregulation of ribosomes is a well established response to cellular stress (López-Maury, Marguerat, & Bähler, 2008), which would be expected during thermal stress and bleaching. Yet, this pattern is not evident in the disease data sets. One explanation for this anomalous pattern may be that this expression reflects an effort by the host to re-establish symbiosis that is repeatedly thwarted either by viral lysis of symbiont cells or bacterial damage to host tissues. An earlier study examining expression during the onset of symbiosis in other coral systems reported upregulation of genes with similar annotations, such as cytoskeleton, cell cycle/growth/differentiation and regulation of transcription (Voolstra, Schnetzer, et al., 2009; Voolstra, Schwarz, et al., 2009), consistent with this hypothesis; however, further work will be needed to determine the precise infection dynamics and host responses, or lack thereof.

Some similarities were evident between the *A. hyacinthus*, *S. siderea*, and *Aiptasia* data sets in the hierarchical clustering of KOG enrichment terms, for example, shared enrichment of inorganic ion transport and metabolism and RNA processing and modification among downregulated genes in *S. siderea* and *Aiptasia*, and cell wall/membrane/envelope biogenesis among downregulated genes in *S. sidera* and *A. hyacinthus*. Yet, it is remarkable how different on average these enrichment patterns are from one another, and from the short-term stress response patterns. Several unique enrichments are evident, for example, the enrichment of intracellular trafficking, secretion, and vesicular transport is unique to *S. siderea* following 95 days of exposure to elevated temperature, while extracellular structures differentiates white syndrome impacted *A. hyacinthus* and menthol-bleached *Aiptasia* is the only data set exhibiting enrichment of amino acid transport and metabolism among upregulated genes. In *S. siderea*, expression responses probably reflect the cellular homeostasis response, rather than a cellular stress response, as

would be expected in the short-term studies. The cellular homeostasis response is secondary to the immediate stress response, and acts to re-establish homeostasis under the new environmental regime (Kültz, 2005). Specific to the environmental perturbation that triggered the initial stress response, the novel patterns of regulation enacted under the homeostasis response persist until another change in environmental conditions occurs. Differential regulation enacted under the cellular homeostasis response is specific to the particular environmental variables that triggered the cellular stress response, and permanent until another change in environmental conditions occurs (Kültz, 2003). Consequently these expression patterns may largely reflect physiological changes necessary to acclimatize to persistently elevated temperature, which occurs in all organisms independent of the algal symbiosis (Schulte, 2015).

Unique patterns among *Aiptasia* KOG term enrichments may reflect the metabolic flexibility of this particular symbiosis, as Symbiodiniaceae are not essential for survival. The divergence in amino acid metabolism may be a reflection of this nutritional independence, where *Aiptasia* may be more capable of regulating their metabolism to make up for a lack of symbiont nutrition than obligately symbiotic scleractinian corals. Early work in another *Aiptasia* species (*pulchella*), showed that Symbiodiniaceae synthesize and translocate seven amino acids to hosts, whereas hosts only synthesized two essential amino acids (Wang & Douglas, 1999). Loss of symbionts, and consequently, a reduction in amino acid supply, may necessitate an upregulation of the host's reliance on heterotrophically derived nutrition, sufficient to meet daily metabolic demand (Hughes & Grottoli, 2013). As *Aiptasia* do not calcify, this upregulation may be sufficient to ensure survival in an aposymbiotic state. Although some scleractinian corals can also shift to heterotrophy during episodes of bleaching to meet metabolic demands (Grottoli, Rodrigues, & Palardy, 2006), no upregulation of genes involved in amino acid metabolism were detected in any other data set (Figure 3d). It is unclear if the *A. millepora* had access to supplemental food, but *S. siderea* were fed brine shrimp throughout the experimental duration (Castillo, Ries, Bruno, & Westfield, 2014) and *P. lobata* were collected directly from their native reef, where polyps comprising both WPS and healthy tissue patches presumably had equal access to food. A multi-species comparison of heterotrophic feeding rates and metabolic shifts following experimental bleaching showed that *P. lobata* was unable to increase heterotrophic metabolism to compensate for symbiont loss (Grottoli et al., 2006). Nutrient stress, potentially resulting from a lack of heterotrophic feeding, was recently shown to result in a novel starvation phenotype in *Aiptasia* (Rädecker et al., 2019), consistent with the idea that heterotrophy may be key to compensating for a lack of symbionts in this system.

Taken together, we observed substantial diversity in global expression responses differentiating stress responses from patterns of symbiont loss, which may help explain the diversity of cellular bleaching mechanisms that have been reported in the literature (Oakley & Davy, 2018; Weis, 2008). As the "omics" revolution continues, additional data sets and greater standardization of methods and reporting (McLachlan, Price, Solomon, & Grottoli, 2020) will contribute to enhancing our understanding of the molecular and cellular processes that distinguish symbiont loss from thermal stress, which will be critical for understanding the mechanistic basis of the mass bleaching crisis.

ACKNOWLEDGEMENTS

The authors are grateful for the field assistance of M. Nayfa, S. Noonan and J. Smith. S. W. Davies, J. L. Matthews and R. M. Wright generously provided access to their raw expression data for the expression meta-analysis. CDK was supported by NSF International Postdoctoral Research Fellowship, DBI-1401165. The Australian Institute of Marine Science supported this work through the use of their research vessel (RV Cape Ferguson) and physiological analysis through internal grants to LKB.

AUTHOR CONTRIBUTIONS

CDK and LKB conceived and designed the experiment. VJLM performed physiological analyses and prepared gene expression libraries. CDK assembled the *P. lobata* transcriptome, conducted gene expression analyses, and drafted the manuscript. All authors contributed to revisions.

DATA AVAILABILITY STATEMENT

Raw tag-seq reads can be obtained from NCBI's SRA under BioProject PRJNA395362 for the WPS expression data set. Raw reads for the *P. lobata* reference transcriptome are available at PRJNA356802. The host transcriptome assembly and associated annotation files are hosted at https://dornsife.usc.edu/labs/carlslab/data/. Bioinformatic and statistical scripts necessary to re-create analyses, as well as raw input data and annotation files used in this study are available at https://github.com/ckenkel/PoritesWPS.

ORCID

Carly D. Kenkel https://orcid.org/0000-0003-1126-4311
Veronique J. L. Mocellin https://orcid.org/0000-0001-9913-302X
Line K. Bay https://orcid.org/0000-0002-9760-2977

REFERENCES

Ainsworth, T. D., & Hoegh-Guldberg, O. (2008). Cellular processes of bleaching in the Mediterranean coral *Oculina patagonica*. *Coral Reefs*, *27*(3), 593–597. https://doi.org/10.1007/s00338-008-0355-x

Anders, S., & Huber, W. (2010). Differential expression analysis for sequence count data. *Genome Biology*, *11*, R106. https://doi.org/10.1186/gb-2010-11-10-r106

Barshis, D. J., Ladner, J. T., Oliver, T. A., Seneca, F. O., Traylor-Knowles, N., & Palumbi, S. R. (2013). Genomic basis for coral resilience to climate change. *Proceedings of the National Academy of Sciences*, *110*(4), 1387–1392. https://doi.org/10.1073/pnas.1210224110

Bieri, T., Onishi, M., Xiang, T., Grossman, A. R., & Pringle, J. R. (2016). Relative contributions of various cellular mechanisms to loss of algae during cnidarian bleaching. *PLoS One*, *11*(4), e0152693. https://doi.org/10.1371/journal.pone.0152693

Brown, B. E., & Howard, L. S. (1985). Assessing the effects of "Stress" on reef corals. *Advances in Marine Biology*, *22*, 1–63.

Bushnell, B. (2014). *BBMap: A Fast, Accurate, Splice-Aware Aligner (No. LBNL-7065E)*. Berkeley, CA: Lawrence Berkeley National Lab. (LBNL). Retrieved from https://www.osti.gov/biblio/1241166-bbmap-fast-accurate-splice-aware-aligner

Castillo, K. D., Ries, J. B., Bruno, J. F., & Westfield, I. T. (2014). The reef-building coral Siderastrea siderea exhibits parabolic responses to ocean acidification and warming. *Proceedings of the Royal Society B: Biological Sciences*, *281*(1797), 20141856. http://dx.doi.org/10.1098/rspb.2014.1856

Chisholm, J. R. M., & Gattuso, J.-P. (1991). Validation of the alkalinity anomaly technique for investigating calcification of photosynthesis in coral reef communities. *Limnology and Oceanography*, *36*(6), 1232–1239. https://doi.org/10.4319/lo.1991.36.6.1232

Crawford, D. R., Wang, Y., Schools, G. P., Kochheiser, J., & Davies, K. J. (1997). Down-regulation of mammalian mitochondrial RNAs during oxidative stress. *Free Radical Biology & Medicine*, *22*(3), 551–559. https://doi.org/10.1016/S0891-5849(96)00380-2

Cziesielski, M. J., Liew, Y. J., Cui, G., Schmidt-Roach, S., Campana, S., Marondedze, C., & Aranda, M. (2018). Multi-omics analysis of thermal stress response in a zooxanthellate cnidarian reveals the importance of associating with thermotolerant symbionts. *Proceedings of the Royal Society B: Biological Sciences*, *285*(1877), 20172654. http://dx.doi.org/10.1098/rspb.2017.2654

Dai, A., Cao, S., Dhungel, P., Luan, Y., Liu, Y., Xie, Z., & Yang, Z. (2017). Ribosome profiling reveals translational upregulation of cellular oxidative phosphorylation mRNAs during vaccinia virus-induced host shutoff. *Journal of Virology*, *91*(5). http://dx.doi.org/10.1128/jvi.01858-16

David, M., Dzamba, M., Lister, D., Ilie, L., & Brudno, M. (2011). SHRiMP2: Sensitive yet practical SHort read mapping. *Bioinformatics*, *27*(7), 1011–1012. https://doi.org/10.1093/bioinformatics/btr046

Davies, S. W., Marchetti, A., Ries, J. B., & Castillo, K. D. (2016). Thermal and pCO2 Stress elicit divergent transcriptomic responses in a resilient coral. *Frontiers in Marine Science*, *3*, 112. https://doi.org/10.3389/fmars.2016.00112

Davy, S. K., Allemand, D., & Weis, V. M. (2012). Cell biology of cnidarian-dinoflagellate symbiosis. *Microbiology and Molecular Biology Reviews*, *76*(2), 229–261. https://doi.org/10.1128/MMBR.05014-11

DeSalvo, M. K., Sunagawa, S., Voolstra, C. R., & Medina, M. (2010). Transcriptomic responses to heat stress and bleaching in the elkhorn coral Acropora palmata. *Marine Ecology Progress Series*, *402*, 97–113. http://dx.doi.org/10.3354/meps08372

DeSalvo, M. K., Voolstra, C. R., Sunagawa, S., Schwarz, J. A., Stillman, J. H., Coffroth, M. A., … Medina, M. (2008). Differential gene expression during thermal stress and bleaching in the Caribbean coral *Montastraea faveolata*. *Molecular Ecology*, *17*(17), 3952–3971.

Dixon, G. B., Davies, S. W., Aglyamova, G. A., Meyer, E., Bay, L. K., & Matz, M. V. (2015). CORAL REEFS. Genomic determinants of coral heat tolerance across latitudes. *Science*, *348*(6242), 1460–1462.

Evans, C., Malin, G., Mills, G. P., & Wilson, W. H. (2006). Viral infection of *Emiliania huxleyi* (prymnesiophyceae) leads to elevated production of reactive oxygen species. *Journal of Phycology*, *42*(5), 1040–1047. https://doi.org/10.1111/j.1529-8817.2006.00256.x

Fitt, W. K., Brown, B. E., Warner, M. E., & Dunne, R. P. (2001). Coral bleaching: Interpretation of thermal tolerance limits and thermal thresholds in tropical corals. *Coral Reefs*, *20*(1), 51–65. https://doi.org/10.1007/s003380100146

Fuess, L. E., Mann, W. T., Jinks, L. R., Brinkhuis, V., & Mydlarz, L. D. (2018). Transcriptional analyses provide new insight into the late-stage immune response of a diseased Caribbean coral. *Royal Society Open Science*, *5*(5), 172062. https://doi.org/10.1098/rsos.172062

Fuess, L. E., Pinzón C, J. H., Weil, E., Grinshpon, R. D., & Mydlarz, L. D. (2017). Life or death: disease-tolerant coral species activate autophagy following immune challenge. *Proceedings of the Royal Society B: Biological Sciences*, *284*(1856), 20170771. http://dx.doi.org/10.1098/rspb.2017.0771

Gates, R. D., Baghdasarian, G., & Muscatine, L. (1992). Temperature stress causes host cell detachment in symbiotic cnidarians: implications for coral bleaching. *The Biological Bulletin*, *182*(3), 324–332. https://doi.org/10.2307/1542252

Gentleman, R., Carey, V., Huber, W., & Hahne, F. (2019). *genefilter: Methods for filtering genes from high-throughput experiments*.

Grabherr, M. G., Haas, B. J., Yassour, M., Levin, J. Z., Thompson, D. A., Amit, I., … Regev, A. (2011). Trinity: Reconstructing a full-length transcriptome without a genome from RNA-Seq data. *Nature Biotechnology*, *29*(7), 644–652.

Grottoli, A. G., Rodrigues, L. J., & Palardy, J. E. (2006). Heterotrophic plasticity and resilience in bleached corals. *Nature*, *440*(7088), 1186–1189.

Huerta-Cepas, J., Forslund, K., Coelho, L. P., Szklarczyk, D., Jensen, L. J., von Mering, C., & Bork, P. (2017). Fast genome-wide functional annotation through orthology assignment by eggNOG-mapper. *Molecular Biology and Evolution*, *34*(8), 2115–2122. https://doi.org/10.1093/molbev/msx148

Huerta-Cepas, J., Szklarczyk, D., Forslund, K., Cook, H., Heller, D., Walter, M. C., … Bork, P. (2016). eggNOG 4.5: A hierarchical orthology framework with improved functional annotations for eukaryotic, prokaryotic and viral sequences. *Nucleic Acids Research*, *44*(D1), D286–D293.

Hughes, A. D., & Grottoli, A. G. (2013). Heterotrophic compensation: A possible mechanism for resilience of coral reefs to global warming or a sign of prolonged stress? *PLoS One*, *8*(11), e81172. https://doi.org/10.1371/journal.pone.0081172

Hughes, T. P., Anderson, K. D., Connolly, S. R., Heron, S. F., Kerry, J. T., Lough, J. M., … Wilson, S. K. (2018). Spatial and temporal patterns of mass bleaching of corals in the Anthropocene. *Science*, *359*(6371), 80–83.

Kauffmann, A., Gentleman, R., & Huber, W. (2009). arrayQualityMetrics–a bioconductor package for quality assessment of microarray data. *Bioinformatics*, *25*(3), 415–416. https://doi.org/10.1093/bioinformatics/btn647

Kenkel, C. D., Aglyamova, G., Alamaru, A., Bhagooli, R., Capper, R., Cunning, R., … Matz, M. V. (2011). Development of gene expression markers of acute heat-light stress in reef-building corals of the genus porites. *PLoS One*, *6*(10), e26914. https://doi.org/10.1371/journal.pone.0026914

Kenkel, C. D., & Bay, L. K. (2017). Novel transcriptome resources for three scleractinian coral species from the Indo-Pacific. *GigaScience*, *6*(9), 1–4. https://doi.org/10.1093/gigascience/gix074

Kenkel, C. D., & Bay, L. K. (2018). Exploring mechanisms that affect coral cooperation: Symbiont transmission mode, cell density and community composition. *PeerJ*, *6*, e6047. https://doi.org/10.7717/peerj.6047

Kenkel, C. D., Moya, A., Strahl, J., Humphrey, C., & Bay, L. K. (2018). Functional genomic analysis of corals from natural CO2 -seeps reveals core molecular responses involved in acclimatization to ocean acidification. *Global Change Biology*, *24*(1), 158–171.

Kenkel, C. D., Sheridan, C., Leal, M. C., Bhagooli, R., Castillo, K. D., Kurata, N., … Matz, M. V. (2014). Diagnostic gene expression biomarkers of coral thermal stress. *Molecular Ecology Resources*, *14*(4), 667–678. https://doi.org/10.1111/1755-0998.12218

Kültz, D. (2003). Evolution of the cellular stress proteome: From monophyletic origin to ubiquitous function. *The Journal of Experimental Biology*, *206*(Pt 18), 3119–3124. https://doi.org/10.1242/jeb.00549

Kültz, D. (2005). Molecular and evolutionary basis of the cellular stress response. *Annual Review of Physiology*, *67*, 225–257. https://doi.org/10.1146/annurev.physiol.67.040403.103635

Lawrence, S. A., Davy, J. E., Wilson, W. H., Hoegh-Guldberg, O., & Davy, S. K. (2015). Porites white patch syndrome: Associated viruses

and disease physiology. *Coral Reefs*, *34*(1), 249–257. https://doi.org/10.1007/s00338-014-1218-2

Lin, S., Cheng, S., Song, B., Zhong, X., Lin, X., Li, W., … Morse, D. (2015). The Symbiodinium kawagutii genome illuminates dinoflagellate gene expression and coral symbiosis. *Science*, *350*(6261), 691–694.

Lin, Z., Chen, M., Dong, X., Zheng, X., Huang, H., Xu, X., & Chen, J. (2017). Transcriptome profiling of *Galaxea fascicularis* and its endosymbiont Symbiodinium reveals chronic eutrophication tolerance pathways and metabolic mutualism between partners. *Scientific Reports*, *7*, 42100. https://doi.org/10.1038/srep42100

Lohman, B. K., Weber, J. N., & Bolnick, D. I. (2016). Evaluation of TagSeq, a reliable low-cost alternative for RNAseq. *Molecular Ecology Resources*, *16*(6), 1315–1321. https://doi.org/10.1111/1755-0998.12529

López-Maury, L., Marguerat, S., & Bähler, J. (2008). Tuning gene expression to changing environments: From rapid responses to evolutionary adaptation. *Nature Reviews Genetics*, *9*(8), 583–593. https://doi.org/10.1038/nrg2398

Matthews, J. L., Crowder, C. M., Oakley, C. A., Lutz, A., Roessner, U., Meyer, E., … Davy, S. K. (2017). Optimal nutrient exchange and immune responses operate in partner specificity in the cnidarian-dinoflagellate symbiosis. *Proceedings of the National Academy of Sciences of the United States of America*, *114*(50), 13194–13199. https://doi.org/10.1073/pnas.1710733114

Matthews, J. L., Sproles, A. E., Oakley, C. A., Grossman, A. R., Weis, V. M., & Davy, S. K. (2016). Menthol-induced bleaching rapidly and effectively provides experimental aposymbiotic sea anemones (Aiptasia sp.) for symbiosis investigations. *The Journal of Experimental Biology*, *219*(Pt 3), 306–310.

McLachlan, R. H., Price, J. T., Solomon, S. L., & Grottoli, A. G. (2020). Thirty years of coral heat-stress experiments: A review of methods. *Coral Reefs*, *39*, 885–902. https://doi.org/10.1007/s00338-020-01931-9

Meyer, E., Aglyamova, G. V., & Matz, M. V. (2011). Profiling gene expression responses of coral larvae (*Acropora millepora*) to elevated temperature and settlement inducers using a novel RNA-Seq procedure. *Molecular Ecology*, *20*(17), 3599–3616. https://doi.org/10.1111/j.1365-294X.2011.05205.x

Mohamed, A. R., Cumbo, V. R., Harii, S., Shinzato, C., Chan, C. X., Ragan, M. A., … Miller, D. J. (2018). Deciphering the nature of the coral-Chromera association. *The ISME Journal*, *12*(3), 776–790. https://doi.org/10.1038/s41396-017-0005-9

Moriya, Y., Itoh, M., Okuda, S., Yoshizawa, A. C., & Kanehisa, M. (2007). KAAS: An automatic genome annotation and pathway reconstruction server. *Nucleic Acids Research*, *35*(Web Server), W182–W185. https://doi.org/10.1093/nar/gkm321

Oakley, C. A., Ameismeier, M. F., Peng, L., Weis, V. M., Grossman, A. R., & Davy, S. K. (2016). Symbiosis induces widespread changes in the proteome of the model cnidarian Aiptasia. *Cellular Microbiology*, *18*(7), 1009–1023.

Oakley, C. A., & Davy, S. K. (2018). Cell Biology of Coral Bleaching. In M. J. H. van Oppen, & J. M. Lough (Eds.), *Coral bleaching: Patterns, processes, causes and consequences* (pp. 189–211). Cham, Switzerland: Springer International Publishing.

Palmer, C. V., & Traylor-Knowles, N. (2012). Towards an integrated network of coral immune mechanisms. *Proceedings of the Royal Society B: Biological Sciences*, *279*(1745), 4106–4114. https://doi.org/10.1098/rspb.2012.1477

Parra, G., Bradnam, K., & Korf, I. (2007). CEGMA: A pipeline to accurately annotate core genes in eukaryotic genomes. *Bioinformatics*, *23*(9), 1061–1067. https://doi.org/10.1093/bioinformatics/btm071

Pinheiro, J., Bates, D., DebRoy, S., Sarkar, D., & Others, (2014). *Linear and nonlinear mixed effects models*. R Package Version, 3. Retrieved from http://ftp.auckland.ac.nz/software/CRAN/doc/packages/nlme.pdf

Polato, N. R., Voolstra, C. R., Schnetzer, J., DeSalvo, M. K., Randall, C. J., Szmant, A. M., … Baums, I. B. (2010). Location-specific responses to thermal stress in larvae of the reef-building coral *Montastraea faveolata*. *PLoS One*, *5*(6), e11221. https://doi.org/10.1371/journal.pone.0011221

Porter, J. W., Fitt, W. K., Spero, H. J., Rogers, C. S., & White, M. W. (1989). Bleaching in reef corals: Physiological and stable isotopic responses. *Proceedings of the National Academy of Sciences of the United States of America*, *86*(23), 9342–9346. https://doi.org/10.1073/pnas.86.23.9342

Pruitt, K. D., Tatusova, T., & Maglott, D. R. (2005). NCBI Reference Sequence (RefSeq): A curated non-redundant sequence database of genomes, transcripts and proteins. *Nucleic Acids Research*, *33*(Database issue), D501–D504.

Quek, Z. B. R., & Huang, D. (2019). Effects of missing data and data type on phylotranscriptomic analysis of stony corals (Cnidaria: Anthozoa: Scleractinia). *Molecular Phylogenetics and Evolution*, *134*, 12–23. https://doi.org/10.1016/j.ympev.2019.01.012

R Development Core Team (2017). *R: A language and environment for statistical computing*. Vienna, Austria: R Foundation for Statistical Computing. Retrieved from https://www.R-project.org/

Rädecker, N., Chen, J. E., Pogoreutz, C., Herrera, M., Aranda, M., & Voolstra, C. R. (2019). Nutrient stress arrests tentacle growth in the coral model Aiptasia. *Symbiosis*, *78*(1), 61–64. https://doi.org/10.1007/s13199-019-00603-9

Raymundo, L. J., Rosell, K. B., Reboton, C. T., & Kaczmarsky, L. (2005). Coral diseases on Philippine reefs: Genus Porites is a dominant host. *Diseases of Aquatic Organisms*, *64*(3), 181–191. https://doi.org/10.3354/dao064181

Ritchie, R. J. (2008). Universal chlorophyll equations for estimating chlorophylls a, b, c, and d and total chlorophylls in natural assemblages of photosynthetic organisms using acetone, methanol, or ethanol solvents. *Photosynthetica*, *46*(1), 115–126. https://doi.org/10.1007/s11099-008-0019-7

Rodriguez-Lanetty, M., Harii, S., & Hoegh-Guldberg, O. (2009). Early molecular responses of coral larvae to hyperthermal stress. *Molecular Ecology*, *18*(24), 5101–5114. https://doi.org/10.1111/j.1365-294X.2009.04419.x

Roff, G., Ulstrup, K. E., Fine, M., Ralph, P. J., & Hoegh-Guldberg, O. (2008). Spatial heterogeneity of photosynthetic activity within diseased corals from the great barrier reef. *Journal of Phycology*, *44*(2), 526–538. https://doi.org/10.1111/j.1529-8817.2008.00480.x

Rogers, A., Blanchard, J. L., & Mumby, P. J. (2014). Vulnerability of coral reef fisheries to a loss of structural complexity. *Current Biology: CB*, *24*(9), 1000–1005. https://doi.org/10.1016/j.cub.2014.03.026

Ruiz-Jones, L. J., & Palumbi, S. R. (2017). Tidal heat pulses on a reef trigger a fine-tuned transcriptional response in corals to maintain homeostasis. *Science Advances*, *3*(3), e1601298. https://doi.org/10.1126/sciadv.1601298

Sawyer, S. J., & Muscatine, L. (2001). Cellular mechanisms underlying temperature-induced bleaching in the tropical sea anemone *Aiptasia pulchella*. *The Journal of Experimental Biology*, *204*(Pt 20), 3443–3456.

Schulte, P. M. (2015). The effects of temperature on aerobic metabolism: Towards a mechanistic understanding of the responses of ectotherms to a changing environment. *The Journal of Experimental Biology*, *218*(Pt 12), 1856–1866. https://doi.org/10.1242/jeb.118851

Shinzato, C., Inoue, M., & Kusakabe, M. (2014). A snapshot of a coral "Holobiont": A transcriptome assembly of the scleractinian coral, porites, captures a wide variety of genes from both the host and symbiotic zooxanthellae. *PLoS One*, *9*(1), e85182. https://doi.org/10.1371/journal.pone.0085182

Shinzato, C., Shoguchi, E., Kawashima, T., Hamada, M., Hisata, K., Tanaka, M., … Satoh, N. (2011). Using the *Acropora digitifera* genome to understand coral responses to environmental change. *Nature*, *476*(7360), 320–323.

Simão, F. A., Waterhouse, R. M., Ioannidis, P., Kriventseva, E. V., & Zdobnov, E. M. (2015). BUSCO: Assessing genome assembly and

annotation completeness with single-copy orthologs. *Bioinformatics*, *31*(19), 3210–3212. https://doi.org/10.1093/bioinformatics/btv351

Stimson, J., & Kinzie, R. A. (1991). The temporal pattern and rate of release of zooxanthellae from the reef coral *Pocillopora damicornis* (Linnaeus) under nitrogen-enrichment and control conditions. *Journal of Experimental Marine Biology and Ecology*, *153*(1), 63–74. https://doi.org/10.1016/S0022-0981(05)80006-1

Strader, M. E., Aglyamova, G. V., & Matz, M. V. (2016). Red fluorescence in coral larvae is associated with a diapause-like state. *Molecular Ecology*, *25*(2), 559–569. https://doi.org/10.1111/mec.13488

Strahl, J., Stolz, I., Uthicke, S., Vogel, N., Noonan, S. H. C., & Fabricius, K. E. (2015). Physiological and ecological performance differs in four coral taxa at a volcanic carbon dioxide seep. *Comparative Biochemistry and Physiology Part A*, *Molecular & Integrative Physiology*, *184*, 179–186. https://doi.org/10.1016/j.cbpa.2015.02.018

Sussman, M., Willis, B. L., Victor, S., & Bourne, D. G. (2008). Coral pathogens identified for White Syndrome (WS) epizootics in the Indo-Pacific. *PLoS One*, *3*(6), e2393. https://doi.org/10.1371/journal.pone.0002393

UniProt Consortium (2015). UniProt: A hub for protein information. *Nucleic Acids Research*, *43*(Database issue), D204–D212.

van de Water, J. A., Chaib De Mares, M., Dixon, G. B., Raina, J.-B., Willis, B. L., Bourne, D. G., & van Oppen, M. J. H. (2018). Antimicrobial and stress responses to increased temperature and bacterial pathogen challenge in the holobiont of a reef-building coral. *Molecular Ecology*, *27*(4), 1065–1080. https://doi.org/10.1111/mec.14489

Voolstra, C. R., Schnetzer, J., Peshkin, L., Randall, C. J., Szmant, A. M., & Medina, M. (2009). Effects of temperature on gene expression in embryos of the coral *Montastraea faveolata*. *BMC Genomics*, *10*, 627. https://doi.org/10.1186/1471-2164-10-627

Voolstra, C. R., Schwarz, J. A., Schnetzer, J., Sunagawa, S., Desalvo, M. K., Szmant, A. M., … Medina, M. (2009). The host transcriptome remains unaltered during the establishment of coral–algal symbioses. *Molecular Ecology*, *18*(9), 1823–1833. https://doi.org/10.1111/j.1365-294X.2009.04167.x

Wang, J. T., & Douglas, A. E. (1999). Essential amino acid synthesis and nitrogen recycling in an alga–invertebrate symbiosis. *Marine Biology*, *135*(2), 219–222. https://doi.org/10.1007/s002270050619

Weis, V. M. (2008). Cellular mechanisms of Cnidarian bleaching: Stress causes the collapse of symbiosis. *The Journal of Experimental Biology*, *211*(Pt 19), 3059–3066. https://doi.org/10.1242/jeb.009597

Weis, V. M. (2019). Cell biology of coral symbiosis: Foundational study can inform solutions to the coral reef crisis. *Integrative and Comparative Biology*, *59*, 845–855. https://doi.org/10.1093/icb/icz067

Wright, R. M., Aglyamova, G. V., Meyer, E., & Matz, M. V. (2015). Gene expression associated with white syndromes in a reef building coral, *Acropora hyacinthus*. *BMC Genomics*, *16*, 371. https://doi.org/10.1186/s12864-015-1540-2

SUPPORTING INFORMATION

Additional supporting information may be found online in the Supporting Information section.

How to cite this article: Kenkel CD, Mocellin VJL, Bay LK. Global gene expression patterns in *Porites* white patch syndrome: Disentangling symbiont loss from the thermal stress response in reef-building coral. *Mol Ecol*. 2020;29:3907–3920. https://doi.org/10.1111/mec.15608